Inorganic Chemistry

Article

pubs.acs.org/IC

Luminescent Properties of Ruthenium(II) Complexes with Sterically Expansive Ligands Bound to DNA Defects

Anna J. McConnell, Mi Hee Lim,† Eric D. Olmon, Hang Song, Elizabeth E. Dervan, and Jacqueline K. Barton*

Division of Chemistry and Chemical Engineering, California Institute of Technology, Pasadena, California 91125, United States

Supporting Information

ABSTRACT: A new family of ruthenium(II) complexes with sterically expansive ligands for targeting DNA defects was prepared, and their luminescent responses to base pair mismatches and/or abasic sites were investigated. Design of the complexes sought to combine the mismatch specificity of sterically expansive metalloinsertors, such as $[Rh(bpy)_2(chrysi)]^{3+}$ (chrysi = chrysene-5,6-quinone diimine), and the light switch behavior of $[Ru(bpy)_2(dppz)]^{2+}$ (dppz = dipyrido[3,2-*a*:2′,3′-*c*]phenazine). In one approach, complexes bearing analogues of chrysi incorporating hydrogen-bonding functionality similar to dppz were synthesized. While the complexes show luminescence only at low temperatures (77 K), competition experiments with $[Ru(bpy)_2(dppz)]^{2+}$ at ambient temperatures reveal that the chrysi derivatives preferentially bind DNA mismatches. In another approach, various substituents were introduced onto the dppz ligand to increase its steric bulk for mismatch binding while maintaining planarity. Steady state luminescence and luminescence lifetime measurements reveal that these dppz derivative complexes behave as DNA "light switches" but that the selectivity in binding and luminescence with mismatched/abasic versus well-matched DNA is not high. In all cases, luminescence depends sensitively upon structural perturbations to the dppz ligand.

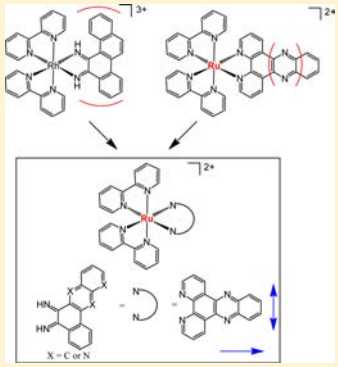

INTRODUCTION

Deficiencies in the DNA mismatch repair pathway, which corrects DNA defects including base pair mismatches and single-base bulges, are associated with several forms of human cancer.[1−3] Our laboratory has been interested in developing octahedral metal complexes that target DNA defects.[4−8] Since deficiencies in mismatch repair necessarily lead to an increased frequency of DNA defects within the cell, targeting these defects with small metal complexes provides a new strategy in designing new cancer diagnostics and chemotherapeutics.

We reported octahedral rhodium complexes that specifically bind single-base mismatch sites in DNA and, upon photoactivation, cleave the DNA backbone.[4−6] The Rh complex $[Rh(bpy)_2(chrysi)]^{3+}$ (Figure 1) recognizes 80% of mismatched sites in all sequence contexts, and selectively targets a single-base mismatch in a 2725 base pair DNA plasmid.[5] Structural studies of the rhodium complex bound to mismatched DNA reveal that it inserts into the destabilized mismatch site from the minor groove with complete ejection of the mismatched base pair into the major groove and no change in base pair rise.[9] Thus, the $[Rh(bpy)_2(chrysi)]^{3+}$ complex is a metalloinsertor rather than a classical metallointercalator. Furthermore, we demonstrated that abasic sites and single-base bulges are also recognized by the $[Rh(bpy)_2(chrysi)]^{3+}$ complex.[10] The source of defect-specific binding is the chrysi-inserting ligand. Structural properties of the chrysi ligand (e.g., steric bulk and planarity) make it too wide to intercalate into well-matched duplex DNA, but it is well suited to bind to destabilized sites in DNA. The binding affinity of this rhodium complex to each mismatch is correlated with the thermodynamic stability of the mismatch.

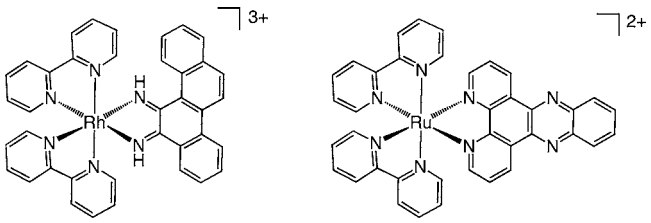

Figure 1. Chemical structures of $[Rh(bpy)_2(chrysi)]^{3+}$and $[Ru(bpy)_2(dppz)]^{2+}$.

Another effort in our laboratory has been constructing metal complexes as luminescent probes for DNA.[8] Complex $[Ru(bpy)_2(dppz)]^{2+}$ (Figure 1, bpy = 2,2′-bipyridine) exhibits light switch behavior in the presence of well-matched DNA.[8] The luminescence of this complex is quenched in aqueous solvents due to formation of hydrogen-bonding interactions between solvent molecules and the phenazine nitrogen atoms of the dppz ligand.[8,11,12] The Ru complex luminesces intensely in the presence of DNA, however, because the phenazine moiety is protected from the quenching environment upon intercalation into the duplex.[8,11,12] Steady state luminescence spectra, excited state lifetime measurements, and NMR studies demonstrate

Received: September 6, 2012
Published: October 31, 2012

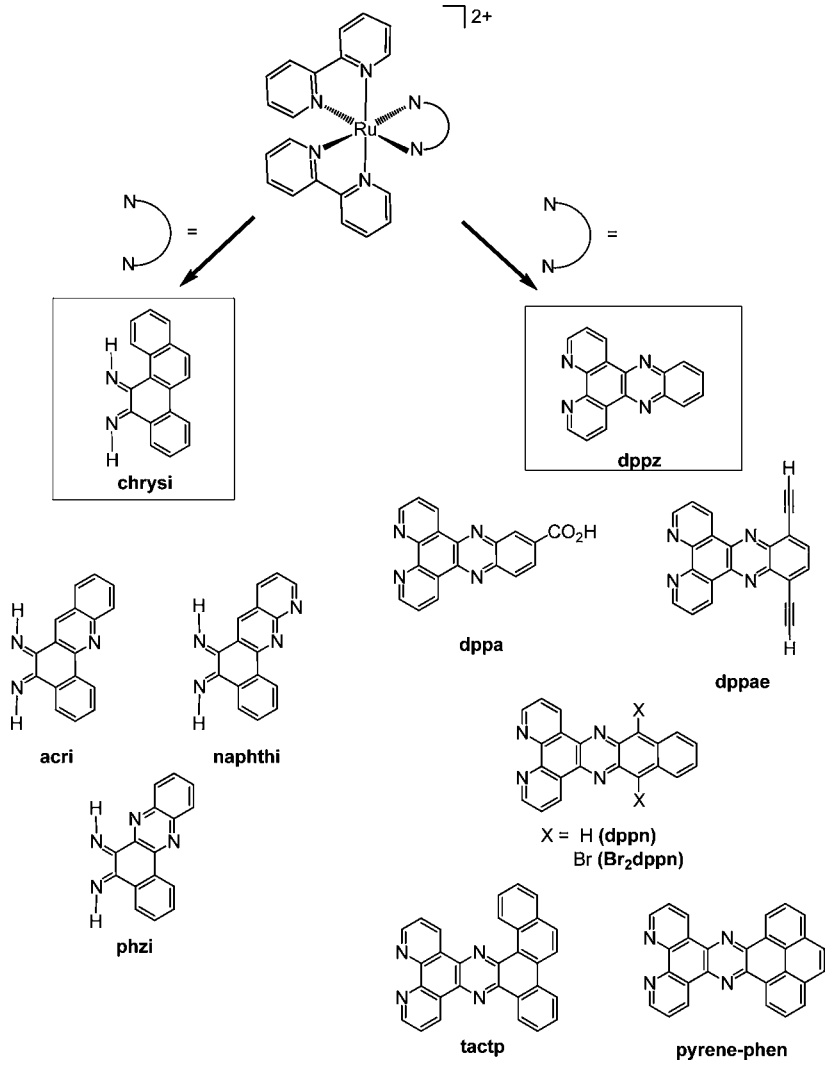

Figure 2. Two strategies for designing new Ru complexes.

that the $[Ru(bpy)_2(dppz)]^{2+}$ complex intercalates into DNA by one of two binding modes: side-on or perpendicular.[8,11,13] In the perpendicular mode, the Ru−dppz axis lies along the DNA dyad axis, protecting the phenazine fragment from water. In the side-on mode, the Ru−dppz axis lies along the long axis of the base stack, partially exposing the ligand to solvent. Thus, complexes bound in the better-protected perpendicular intercalation mode show greater luminescent enhancement upon binding to DNA and have longer excited state lifetimes than those in the side-on mode. Recent crystal structures have shown intercalation of dppz complexes into the DNA duplex from the minor groove,[14,15] though NMR studies have pointed to intercalation from the major groove;[13] the energetic differences between major and minor groove orientations must be small.

How might the luminescent properties of the $[Ru(bpy)_2(dppz)]^{2+}$ complex change in the presence of DNA containing a defect? Previously, we have shown that $[Ru(bpy)_2(dppz)]^{2+}$, while showing luminescence bound to duplex DNA, shows still greater luminescence in the presence of a mismatch.[16] More recent efforts to understand how mismatches affect $[Ru(bpy)_2(dppz)]^{2+}$ binding have led to determination of an atomic-resolution crystal structure of Δ-$[Ru(bpy)_2(dppz)]^{2+}$ bound to a mismatch-containing oligonucleotide.[14] The structure reveals that, like its rhodium counterpart, the ruthenium complex also recognizes the destabilized mismatches through metalloinsertion: the dppz ligand inserts into the base stack from the minor groove, extruding the mispaired bases out of the helix. Thus, it is conceivable that by combining the structural features of $[Rh(bpy)_2(chrysi)]^{3+}$ (for mismatch-specific recognition) and $[Ru(bpy)_2(dppz)]^{2+}$ (for luminescence) it might be possible to develop an improved luminescent reporter for DNA defects. Here, we investigated two approaches for enhancing the mismatch specificity: (i) replacement of the dppz ligand with sterically expansive inserting ligands, such as chrysi, and (ii) incorporation of various functionalities onto the dppz ligand to increase the steric bulk. We report the preparation of a new family of $[Ru(bpy)_2(L)]^{2+}$ derivatives (Figure 2) and the luminescent behavior of each derivative in the presence of duplex DNA with and without defects.

EXPERIMENTAL PROCEDURES

Materials and Methods. All reagents and solvents were purchased from commercial suppliers and used without further purification. Chrysene-5,6-quinone and benzo[*a*]phenazine-5,6-quinone were synthesized according to literature procedures.[17] Ru complexes $Ru(bpy)_2Cl_2$, $[Ru(bpy)_2(dppz)](X)_2$ (**15**), and $[Ru(bpy)_2(tactp)](X)_2$ (**18**, X = PF_6 or Cl) were prepared by previously

dx.doi.org/10.1021/ic3019524 | *Inorg. Chem.* 2012, 51, 12511−12520

described procedures.[8,18,19] UV−vis spectra were recorded on a Beckman DU 7400 UV−visible spectrophotometer (Beckman Coulter). Oligonucleotides 5′-GAC CAG CTT ATC ACC CCT AGA TAA GCG-3′ and 3′- CTG GTC GAA TAG TXG GGA TCT ATT CGC-5′ [X = G (M), C (MM), or R (AB, R denotes a tetrahydrofuranyl abasic site)] were synthesized on an ABI 3400 DNA synthesizer (Applied Biosystems) or purchased from Integrated DNA Technologies and purified as previously reported.[20]

Synthesis. *1,2-Dihydrobenz[c]acridine (1).* This compound was synthesized according to the literature procedure[21] and purified by SiO_2 column chromatography (9:1 hexane/EtOAc). Yield: 57%. ^{1}H NMR ($CDCl_3$, 300 MHz, δ (ppm)): 8.60 (d, ^3J = 7.4 Hz, 1H), 8.17 (d, ^3J = 8.3 Hz, 1H), 7.95 (s, 1H), 7.77 (d, ^3J = 8.1 Hz, 1H), 7.67 (t, ^3J = 7.6 Hz, 1H), 7.59−7.33 (m, 3H), 7.33−7.25 (m, 1H), 3.15 (t, ^3J = 6.5 Hz, 2H), 3.03 (t, ^3J = 6.5 Hz, 2H). ESI(+)MS (m/z): $[M+H]^+$ calcd 232.1, found, 232.4.

5,6-Dihydronaphtho[1,2-b][1,8]naphthyridine (2). A suspension of α-tetralone (0.39 g, 2.7 mmol), (2-aminopyridin-3-yl)methanol[22] (0.33 g, 2.6 mmol), benzophenone (0.48 g, 2.6 mmol), and potassium *tert*-butoxide (0.30 g, 2.7 mmol) in dry dioxane (10 mL) was heated under reflux under an Ar atmosphere for 2 h. The red suspension was cooled to room temperature, filtered through Celite, and poured into a saturated NH_4Cl solution (20 mL). This was extracted with EtOAc (3 × 20 mL), and the combined organic layers were dried over Na_2SO_4 and filtered, and solvent was removed. Crude material was purified by SiO_2 column chromatography (1:1 hexane/EtOAc) to give **2** as a pale red solid (0.37 g, 61%). ^{1}H NMR ($CDCl_3$, 300 MHz, δ (ppm)): 9.06 (dd, ^3J = 4.2 Hz, ^4J = 1.8 Hz, 1H), 8.84−8.73 (m, 1H), 8.20−8.05 (m, 1H), 7.95 (s, 1H), 7.50−7.35 (m, 3H), 7.33−7.23 (m, 1H), 3.29−3.09 (m, 2H), 3.10−2.96 (m, 2H). ESI(+)MS (m/z): $[M + H]^+$ calcd 233.1, found 233.4; $[2M + Na]^+$ calcd 487.2, found 486.9.

Ligand 3 and 4 Synthesis. A solution of **1** or **2** (2.0 mmol) in 1:1 acetic acid/acetic anhydride (10 mL) was cooled in an ice bath (Scheme 1). A solution of $Na_2Cr_2O_7$ (0.90 g, 3.0 mmol) in 1:1 acetic

Scheme 1

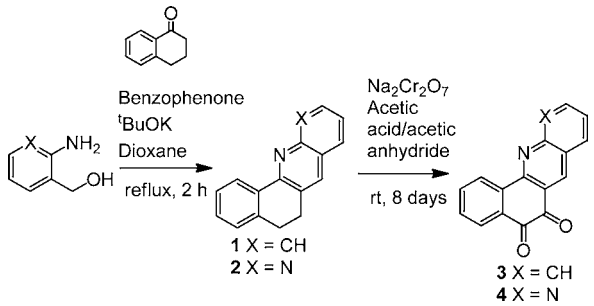

acid/acetic anhydride (10 mL) was added dropwise, and the reaction mixture was allowed to warm to room temperature. The reaction was stirred at room temperature for 8 days, during which time a yellow solid precipitated from the reaction mixture. Yellow precipitate was filtered, washed with H_2O, and dried.

Benz[c]acridine (acri) Quinone (3).[23] Yield: 81%. ^{1}H NMR ($CDCl_3$, 300 MHz, δ (ppm)): 9.07−8.87 (m, 2H), 8.25 (t, ^3J = 8.1 Hz, 1H), 8.19 (d, ^3J = 8.4 Hz, 1H), 7.98 (d, ^3J = 8.1 Hz, 1H), 7.89 (dd, ^3J = 16.4, 8.1 Hz, 2H), 7.64 (t, ^3J = 7.4 Hz, 2H). ESI(+)MS (m/z): $[2M + Na]^+$ calcd 541.1, found 540.8.

5,6-Naphtho[1,2-b][1,8]naphthyridine (naphthi) Quinone (4). Yield: 69%. ^{1}H NMR ($CDCl_3$, 300 MHz, δ (ppm)): 9.29 (dd, ^3J = 4.1 Hz, ^4J = 1.8 Hz, 1H), 9.11 (d, ^3J = 7.9 Hz, 1H), 9.06 (s, 1H), 8.38 (dd, ^3J = 8.1 Hz, ^4J = 1.7 Hz, 1H), 8.30 (d, ^3J = 7.6 Hz, 1H), 7.91 (t, ^3J = 7.4 Hz, 1H), 7.69 (t, ^3J = 7.5 Hz, 1H), 7.62 (dd, ^3J = 8.1, 4.2 Hz, 1H). ESI(+)MS (m/z): $[M + CH_3OH + H]^+$ calcd 293.1, found 293.1.

3,6-Diethynylbenzene-1,2-diamine (7). A solution of 4,7-diethynylbenzo[*c*][1,2,5]-thiadiazole[24] (200 mg, 1.1 mmol) in 30 mL of THF was purged with Ar for 30 min and cooled to 0 °C. Eight equivalents of $LiAlH_4$ (in THF) were added dropwise over 10 min. The resulting solution was stirred for 10 min at 0 °C and allowed to warm slowly to room temperature. The reaction was quenched by addition of water after stirring for 4 h at room temperature, and the solution was filtered. Filtrate was extracted with CH_2Cl_2 (three times). After removal of CH_2Cl_2, the crude product was purified by SiO_2 column chromatography with a solvent gradient (50%:50% Hx:CH_2Cl_2 to 100% CH_2Cl_2) to obtain the desired product **7** (153 mg, 0.98 mmol, 89%). ^{1}H NMR ($CDCl_3$, 300 MHz, δ (ppm)): 6.82 (s, 2H), 3.98 (br, s, 4H), 3.44 (s, 2H). HREI (m/z) for M^+ calcd 156.0687, found 156.0687.

1,4-Dibromo-2,3-diaminonaphthalene (9). **9** was synthesized according to reported procedures.[25]

Dppz Derivatives. Ligands were synthesized by refluxing **5**−**9** (0.63 mmol) with 1,10-phenanthroline-5,6-dione and **10** or **11** with 5,6-diamino-1,10-phenanthroline[26] (0.63 mmol) in ethanol (10 mL) for 8 h, as shown in Scheme 2.[8d] Yellow precipitates were collected, washed with cold ethanol (three times, 20 mL), dried under vacuum, and used for preparation of the Ru complexes without further purification.

Dppa. Yield: 86%. ESI(+)MS (m/z): $[M + H]^+$ calcd 327.1, found 327.2.

Dppae. Yield: 40%. ESI(+)MS (m/z): $[M + H]^+$ calcd 331.1, found 331.2.

Dppn. Yield: 83%. ESI(+)MS (m/z): $[M + H]^+$ calcd 333.1, found 333.1.

Br_2dppn. Yield: 75%. ESI(+)MS (m/z): $[M + H]^+$ calcd 490.9, found 491.0.

Pyrene-phen. Yield: 90%. ESI(+)MS (m/z): $[M + H]^+$ calcd 407.1, found 407.3.

$[Ru(bpy)_2(NH_3)_2](PF_6)_2$. A solution of $Ru(bpy)_2Cl_2$ (0.47 g, 0.9 mmol) and NH_4OH (10 mL) in MeOH (5 mL) was heated at 60 °C for 4 h. The reaction mixture was cooled to room temperature, and the solvent was removed in vacuo. Residue was redissolved in MeOH and precipitated with Et_2O. Solid was collected and redissolved in water (10 mL), and excess NH_4PF_6 (s) was added. The suspension was stirred in the absence of light for 1 h and filtered, and the red precipitate was washed with cold water (15 mL) and Et_2O (3 × 10 mL) and dried under vacuum to give $[Ru(bpy)_2(NH_3)_2](PF_6)_2$ (0.58 g, 0.8 mmol, 88%). ^{1}H NMR (CD_3OD, 300 MHz, δ (ppm)): 9.18 (d, ^3J = 5.6 Hz, 2H), 8.64 (d, ^3J = 8.1 Hz, 2H), 8.46 (d, ^3J = 8.1 Hz, 2H), 8.20 (t, ^3J = 7.9 Hz, 2H), 7.82 (t, ^3J = 7.7 Hz, 4H), 7.65 (d, ^3J = 5.7 Hz, 2H), 7.27−7.08 (m, 2H), 2.89 (s, 6H).

$[Ru(bpy)_2(L)]^{2+}$ Complexes. *Method 1.* A suspension of $[Ru(bpy)_2(NH_3)_2](PF_6)_2$ (0.043 mmol) and NaH (0.8 mmol) in dry MeCN (10 mL) was deoxygenated and stirred under an Ar atmosphere for 30 min. Ligand (0.048 mmol) was added; the mixture was deoxygenated and stirred at room temperature for 4 h before quenching the reaction with a couple of drops of 1 M HCl. The reaction mixture was diluted with water (10 mL), excess NH_4PF_6 (s) was added, and the solution was concentrated in vacuo. Precipitates were collected and washed with water (2 × 10 mL) and then converted to the soluble chloride salt by anion exchange chromatography (Sephadex QAE). Residues were purified on a Waters C_{18} sep-pak cartridge and by preparative HPLC using a gradient of H_2O (with 0.1% TFA) to CH_3CN over 60 min. Complex was converted to the chloride salt by anion exchange chromatography (Sephadex QAE).

$[Ru(bpy)_2(chrysi)](X)_2$ (12, X = TFA or Cl). Yield: 18%. ^{1}H NMR (CD_3CN, 300 MHz, δ (ppm)): 12.91 (s, 1H), 12.42 (s, 1H), 8.58−8.44 (m, 7H), 8.39−8.30 (m, 1H), 8.24 (d, ^3J = 8.8 Hz, 1H), 8.19−8.03 (m, 5H), 7.94 (d,^{3} J = 5.6 Hz, 2H), 7.82 (t, ^3J = 8.3 Hz, 1H), 7.73−7.59 (m, 5H), 7.54−7.39 (m, 4H). ESI(+)MS (m/z): $[M - H]^+$ calcd 669.1, found 669.1; $[M]^{2+}$ calcd 335.1, found 334.6. UV−vis in H_2O, λ_{abs}/nm ($\varepsilon \times 10^4/M^{-1}$ cm^{-1}): 255 (11.5), 282 (14.5), 550 (6.4).

$[Ru(bpy)_2(acri)](X)_2$ (13, X = TFA or Cl). Yield: 22%. ^{1}H NMR (CD_3CN, 300 MHz, δ (ppm)): 14.06 (s, 1H), 13.07 (s, 1H), 9.75 (s, 1H), 9.12 (dd, ^3J = 8.1 Hz, ^4J = 1.4 Hz, 1H), 8.60−8.44 (m, 5H), 8.19 (d, ^3J = 8.6 Hz, 1H), 8.13−8.00 (m, 7H), 7.97−7.84 (m, 1H), 7.83 (t, ^3J = 7.6 Hz, 1H), 7.76−7.59 (m, 4H), 7.54−7.37 (m, 4H). ESI(+)MS (m/z): $[M - H]^+$ calcd 670.1, found 670.3; $[M]^{2+}$ calcd 335.6, found

dx.doi.org/10.1021/ic3019524 | *Inorg. Chem.* 2012, 51, 12511−12520

Scheme 2

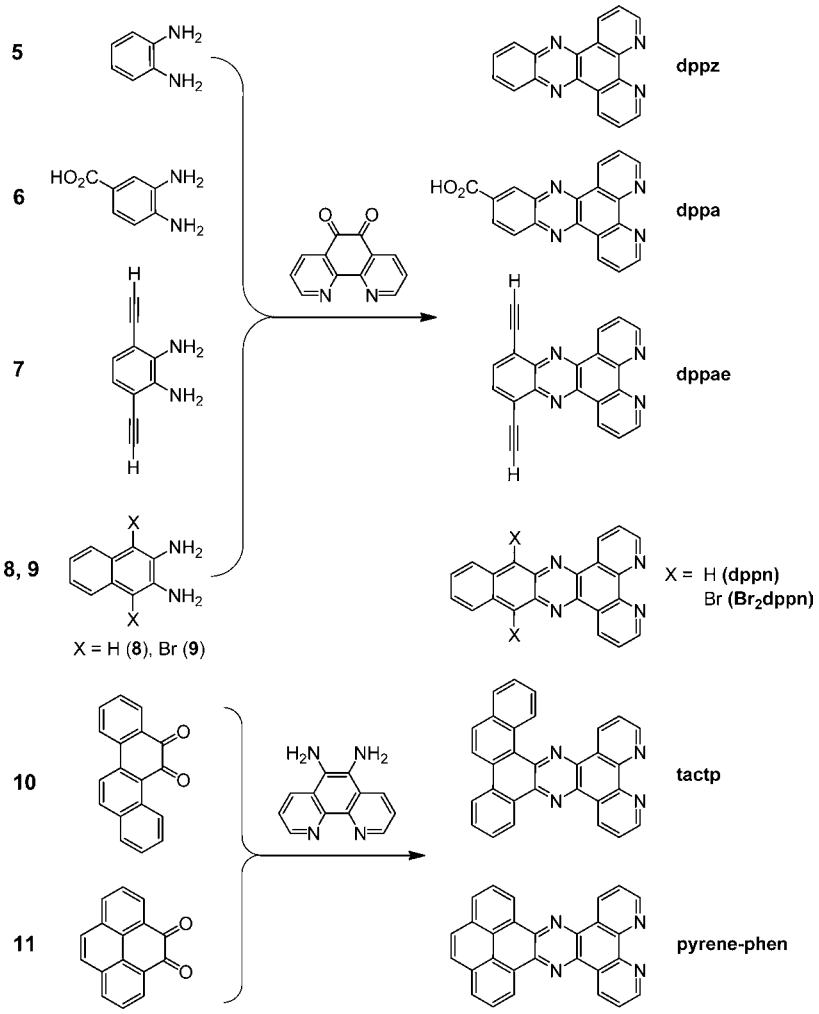

335.7. UV−vis in H_2O, λ_{abs}/nm ($\varepsilon \times 10^4/M^{-1}$ cm^{-1}): 238 (5.1), 285 (8.2), 400 (1.1), 438 (1.2), 542 (3.7).

[Ru(bpy)$_2$(naphthi)](X)$_2$ (**14**, *X = TFA or Cl*). Yield: 4%. ^{1}H NMR (CD_3CN, 300 MHz, δ (ppm)): 13.76 (s, 1H), 12.79 (s, 1H), 9.62 (s, 1H), 9.21 (dd, ^3J = 4.1 Hz, ^4J = 1.9 Hz, 1H), 9.08 (d, ^3J = 7.4 Hz, 1H), 8.58−8.38 (m, 6H), 8.07 (dd, ^3J = 16.0, 8.0 Hz, 6H), 7.89−7.58 (m, 5H), 7.54−7.31 (m, 4H). ESI(+)MS (m/z): $[M - H]^+$ calcd 671.1, found 671.2; $[M]^{2+}$ calcd 336.1, found 335.4. UV−vis in H_2O, λ_{abs}/nm ($\varepsilon \times 10^4/M^{-1}$ cm^{-1}): 241 (4.6), 288 (6.8), 425 (1.1), 540 (2.7).

Method 2. Ethylene glycol (7 mL) was added to a mixture of $Ru(bpy)_2Cl_2$ (0.069 mmol) and the dppz derivatives (0.069 mmol), and the solution was heated to 130 °C for 12 h (Scheme 3). After cooling the reaction mixture to room temperature, the solution was diluted with water (7 mL) followed by addition of excess NH_4PF_6 (s). Orange precipitates were collected, washed with water (3 × 5 mL), and dried under vacuum. Complexes were recrystallized by addition of Et_2O into their CH_3CN solutions at room temperature and afterward converted to the soluble Cl salt by anion exchange chromatography (Sephadex QAE). They were further purified by preparative HPLC using a gradient of H_2O (with 0.1% TFA) to CH_3CN (with 0.1% TFA) over 30 min.

[Ru(bpy)$_2$(dppa)](X)$_2$ (**16**, *X = PF$_6$ or Cl*). Yield: 63%. ^{1}H NMR (CD_3CN, 500 MHz, δ (ppm)): 9.76−9.68 (m, 2H), 9.06 (m, 1H), 8.70 (m, 1H), 8.59−8.54 (m, 4H), 8.49 (1H, m), 8.22 (s, br, 2H), 8.14 (m, 2H), 8.05 (m, 2H), 7.94 (m, 2H), 7.89 (m, 2H), 7.79 (2H, m), 7.49 (m, 2H), 7.30 (m, 2H). ESI(+)MS (m/z): $[M - 2(PF_6)]^{2+}$ calcd 370.1, found 370.0; $[M - PF_6]^+$ calcd 885.1, found 885.2. UV−vis in H_2O, λ_{abs}/nm ($\varepsilon \times 10^4/M^{-1}$ cm^{-1}): 284 (10), 362 (1.9), 378 (1.9), 444 (1.6).

Scheme 3

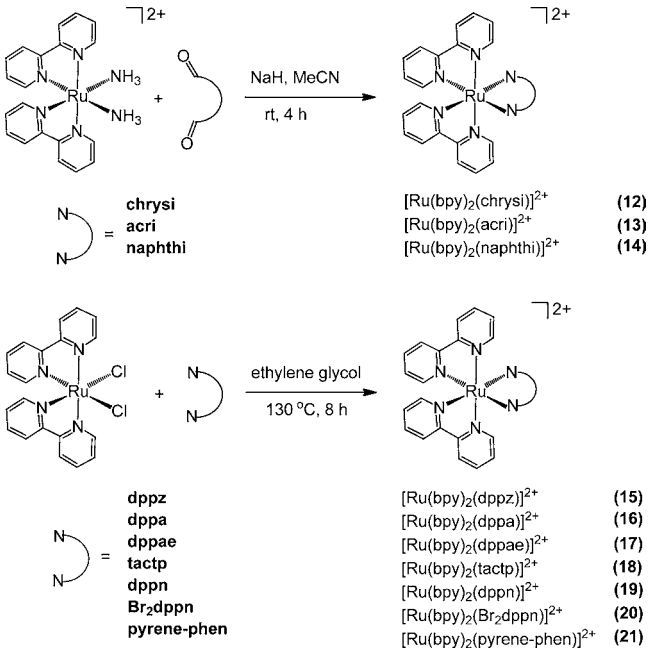

dx.doi.org/10.1021/ic3019524 | *Inorg. Chem.* 2012, 51, 12511−12520

*[Ru(bpy)$_2$(dppae)](X)$_2$ (**17**).* Ru complex was prepared as described above. Crude product was purified via preparative TLC (silica, 4:4.5:1, CH_3CN:water:NH_4Cl (satd, aq)) followed by preparative HPLC (a gradient of H_2O with 0.1% TFA to CH_3CN with 0.1% TFA). Cl salt was then obtained using anion exchange chromatography on Sephadex QAE. Yield: 20%. ESI(+)MS (m/z): $[M - 2(Cl)]^{2+}$ calcd 372.1, found 372.0. UV−vis in H_2O, λ_{abs}/nm ($\varepsilon \times 10^4/M^{-1}$ cm^{-1}): 244 (4.3), 272 (sh, 4.7), 288 (6.3), 306 (4.3), 364 (1.2), 380 (1.5), 426 (1.4), 440 (1.3).

*[Ru(bpy)$_2$(dppn)](X)$_2$ (**19**).* Yield: 72%. ^{1}H NMR (CD_3CN, 500 MHz, δ (ppm)): 9.71−9.681 (m, 2H), 9.17−9.16 (m, 2H), 8.57 (dd, J = 8.0 Hz, 4H), 8.41−8.39 (m, 2H), 8.18−8.14 (m, 4H), 8.10−8.05 (m, 2H), 7.94−7.88 (m, 4H), 7.82−7.78 (m, 4H), 7.52−7.49 (m, 2H), 7.34−7.31 (m, 2H). ESI(+)MS (m/z): $[M - 2(PF_6)]^{2+}$ calcd 373.1, found 373.1; $[M - PF_6]^+$ calcd 891.1, found 891.2. UV−vis in H_2O, λ_{abs}/nm ($\varepsilon \times 10^4/M^{-1}$ cm^{-1}): 244 (5.3), 286 (7.0), 324 (7.4), 390 (1.6), 412 (2.2), 442 (2.0).

*[Ru(bpy)$_2$(Br$_2$dppn)](X)$_2$ (**20**).* Yield: 69%. ^{1}H NMR (CD_3CN, 500 MHz, δ (ppm)): 8.43−8.41 (m, 2H), 7.49−7.46 (m, 2H), 7.43−7.39 (m, 4H), 6.96−6.94 (m, 2H), 6.87−6.84 (m, 2H), 6.79−6.76 (m, 2H), 6.66−6.55 (m, 8H), 6.23 (2H, m), 6.06 (2H, m). ESI(+)MS (m/z): $[M - 2(PF_6)]^{2+}$ calcd 451.0, found 451.0; $[M - PF_6]^+$ calcd 1049.3, found 1049.1. UV−vis in H_2O, λ_{abs}/nm ($\varepsilon \times 10^4/M^{-1}$ cm^{-1}): 254 (3.7), 286 (4.5), 324 (4.3), 396 (1.0), 420 (1.4), 446 (1.4).

*[Ru(bpy)$_2$(pyrene-phen)](X)$_2$ (**21**).* Yield: 76%. ^{1}H NMR (CD_3CN, 500 MHz, δ (ppm)): 9.71 (d, ^3J = 7.5 Hz, 2H), 9.47 (d, ^3J = 7.5 Hz, 2H), 8.59 (t, ^3J = 9.3 Hz, 4H), 8.27−8.23 (m, 4H), 8.19−8.11 (m, 4H), 8.06 (td, ^3J = 8.0 Hz, ^4J = 1.2 Hz, 2H), 8.0−7.92 (m, 4H), 7.84 (d, ^3J = 5.1 Hz, 2H), 7.74 (s, 2H), 7.52 (m, 2H), 7.34 (m, 2H). ESI(+)MS (m/z): $[M - 2(PF_6)]^{2+}$ calcd 410.8, found 410.2; $[M - PF_6]^+$ calcd 965.1, found 965.4. UV−vis in H_2O, λ_{abs}/nm ($\varepsilon \times 10^4/M^{-1}$ cm^{-1}): 236 (3.7), 288 (5.0), 348 (1.1), 452 (1.3), 476 (1.3).

Luminescence Measurements. *Steady State Fluorescence.* Luminescence spectra were recorded on an ISS-K2 spectrofluorometer in 5 mM Tris, 50 mM NaCl, pH 7.5 at ambient temperature or in a 10 M LiCl glass at 77 K in aerated solutions. Samples were excited at 440 nm, and the emission intensity was integrated from 560 to 800 nm.

Excited State Lifetime Measurements. Samples were excited using a Nd:YAG-pumped OPO (Spectra-Physics Quanta-Ray). Laser power at 470 nm ranged from 3.0 to 4.5 mJ per pulse at 10 Hz. Emitted light was collected and focused onto the entrance slit of an ISA double-grating (100 mm) monochromator and detected by a PMT (Hamamatsu R928). Each measurement is the average of 500 or 1000 shots of 8 ns duration. Emission decays were fit to mono- or biexponential functions using nonlinear least-squares minimization.

RESULTS AND DISCUSSION

Design Considerations. Inspired by the activity of $[Rh(bpy)_2(chrysi)]^{3+}$ and $[Ru(bpy)_2(dppz)]^{2+}$ (Figure 1) toward DNA,[4−10,13,14,16] we aimed to develop a new framework for detecting DNA defects based on luminescence. The key feature of the chrysi complex that enables it to specifically bind to destabilized sites in DNA is the sterically expansive inserting chrysi ligand.[4−7,9,10] Meanwhile, the luminescence-based detection of DNA by $[Ru(bpy)_2(dppz)]^{2+}$ is based on the protection of the dppz ligand from water by the DNA duplex.[8,13] Thus, by combining the characteristics of chrysi and dppz into a single ligand, it may be possible to create a Ru complex that luminesces only when specifically bound to DNA defects. Guided by these design considerations, a series of ruthenium complexes, based on the structures of both $[Rh(bpy)_2(chrysi)]^{3+}$ and $[Ru(bpy)_2(dppz)]^{2+}$ using two strategies, was prepared as candidate luminescent reporters for DNA defects (Figure 2). In one approach, sterically expansive chrysi analogues with hydrogen-bonding functionality similar to the dppz ligand were investigated. The chrysi parent complex was also studied as a comparison; this complex was not expected to show "light-switch" behavior but specificity in binding a mismatch was expected due to the ligand expanse.

In the second approach, simple substitutions (CO_2H, acetylene, Br, and phenyl) were incorporated onto the dppz ligand in order to increase its width, length, or both (Figure 2). For example, the wider ligand framework in pyrene-phen and tactp is similar to that of the sterically bulky chrysi ligand. As dppn is longer than dppz, $[Ru(bpy)_2(dppn)]^{2+}$ will likely bind to well-matched sites from the major groove rather than the minor groove leading to greater exposure of the phenazine nitrogen atoms to solvent compared to dppz, thus reducing luminescence. Therefore, because of the likelihood of low luminescence when bound to well-matched DNA, complexes with dppn (or dppa) might show a significant increase in luminescence due only to selective intercalation or insertion into destabilized lesion sites in DNA. Alternatively, increasing the width of the dppz ligand to make dppae or tactp was expected to discourage the binding of the complex to well-matched DNA in a similar fashion to the sterically expansive chrysi ligand. Increasing both the length and the width (to make Br_2dppn and pyrene-phen) would then combine the effects.

Synthesis of the Ru Complexes. Ligands **1** and **2** were synthesized in two steps from α-tetralone by a Friedländer synthesis and subsequent oxidation with sodium dichromate (Scheme 1).[21,23] Ruthenium complexes **12**−**14** were synthesized by reacting $[Ru(bpy)_2(NH_3)_2](PF_6)_2$ with the appropriate quinone ligand in the presence of sodium hydride at ambient temperature (Scheme 3). Complexes **12**−**14** were isolated in 4−20% yield following purification and anion exchange to the chloride salt. Unexpectedly, $[Ru(bpy)_2(phzi)]^{2+}$ (Figure 2) was not the major product from the reaction with benzo[*a*]phenazine-5,6-quinone and was only isolated in trace amounts, as characterized by HPLC and mass spectrometry. We propose that $[Ru(bpy)_2(iqi)]^{2+}$ (**22**) (Figure S1, Supporting Information) is the major product of the reaction as the ^{1}H NMR spectrum of the isolated complex only contains one imine proton signal, and the mass spectrum is consistent with loss of carbon monoxide. It has been reported that a related ligand, 1,10-phenanthroline-5,6-dione, loses carbon monoxide under basic conditions.[27] Similar ligand decomposition in the presence of sodium hydride during the course of the reaction could account for the low yields of complexes **12**−**14**[28] and formation of byproduct **22**. Following the loss of carbon monoxide from benzo[*a*]phenazine-5,6-quinone, unlike the other ligands, it is still possible to coordinate to the metal center in a bidentate fashion through the phenazine nitrogen and imine formed from the remaining quinone.

Ru complexes $[Ru(bpy)_2(dppz)]^{2+}$ (**15**) and $[Ru(bpy)_2(tactp)]^{2+}$ (**18**) were prepared by previously published methods.[8,19] For the ligands dppa, dppae, dppn, and Br_2dppn (Scheme 2), the amine moieties were condensed with 1,10-phenanthroline-5,6-dione in ethanol.[8d,24,25] The pyrene-phen ligand was obtained by condensation of pyrene-4,5-dione and 5,6-diamino-1,10-phenanthroline[26] in ethanol.[8d] Complexes (**16**, **17**, and **19**−**21**) were obtained by refluxing a solution containing $Ru(bpy)_2Cl_2$ and 1 equiv of the corresponding dppz derivative in ethylene glycol at 130 °C for 8 h, as depicted in Scheme 3. Addition of excess NH_4PF_6 (s) into the reaction solution of 1:1 ethylene glycol:water allowed isolation of the Ru complexes as PF_6 salts, followed by purification via recrystallization or column chromatography. All complexes show the

dx.doi.org/10.1021/ic3019524 | *Inorg. Chem.* 2012, 51, 12511−12520

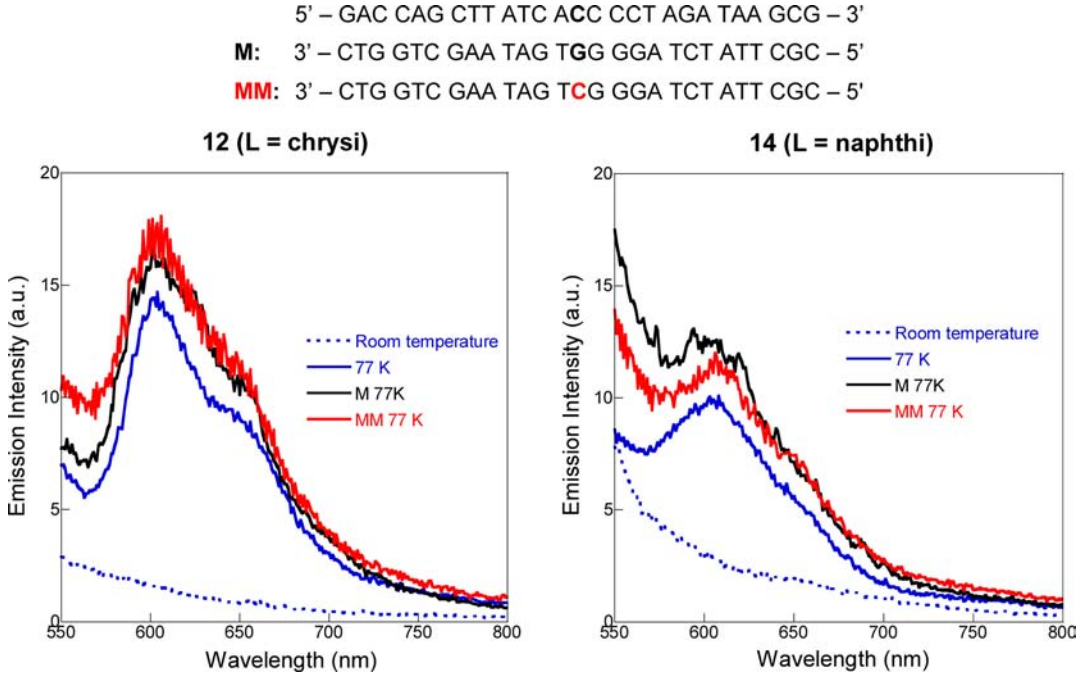

Figure 3. Emission spectra of $[Ru(bpy)_2(chrysi)]^{2+}$ (**12**) and $[Ru(bpy)_2(naphthi)]^{2+}$ (**14**) in the presence and absence of DNA at 77 K and room temperature (10 M LiCl, λ_{ex} = 440 nm). [Ru] = 5 μM, [DNA] = 0 or 5 μM. DNA sequences are shown at the top of the figure.

characteristic MLCT transition absorption in the visible region at ~440 nm.

Luminescent Characteristics of the Ru Complexes with and without DNA. While complexes **12**–**14** (Scheme 3 and Figure 2) are not luminescent at ambient temperature in various solvents (dry MeCN, Tris buffer, and 10 M LiCl), $[Ru(bpy)_2(chrysi)]^{2+}$ (**12**) and $[Ru(bpy)_2(naphthi)]^{2+}$ (**14**) are luminescent in the absence of DNA at 77 K in a 10 M LiCl glass (Figure 3). In the presence of DNA, there is no luminescence differential between mismatched and matched DNA for both complexes. $[Ru(bpy)_2(acri)]^{2+}$ (**13**) is not luminescent at 77 K in dry MeCN nor in the presence or absence of DNA in 10 M LiCl upon excitation at 440 nm. The DNA "light switch" complex $[Ru(bpy)_2(dppz)]^{2+}$ (**15**) is also luminescent at 77 K in the absence of DNA (Figure S2, Supporting Information). Therefore, it is not possible to determine the mismatch specificity or light switch behavior of the complexes from low-temperature experiments.

At ambient temperature, $[Ru(bpy)_2(chrysi)]^{2+}$ (**12**), $[Ru(bpy)_2(acri)]^{2+}$ (**13**), and $[Ru(bpy)_2(naphthi)]^{2+}$ (**14**) are not luminescent in the absence or presence of DNA. Therefore, competition experiments were carried out with the "light switch" complex $[Ru(bpy)_2(dppz)]^{2+}$ (**15**) in order to investigate the room-temperature mismatch specificity of the complexes. Control experiments reveal that complexes **12**–**14** do not quench the luminescence of **15** in the absence of DNA in dry MeCN (Figure S3, Supporting Information). Luminescence of 1:1 DNA/**15** mixtures in aqueous buffer was measured upon addition of up to 10 equiv of complexes **12**–**14**. A decrease in the luminescence is expected if the complex displaces **15**, as **15** is luminescent only when bound to DNA. For all three complexes **12**–**14**, there was a small decrease in the luminescence of **15** in the presence of matched DNA with the largest decrease observed with **12** (33% after 1 equiv). In contrast, there was a much more significant luminescence decrease, following the order **12** (55% after 1 equiv) > **13** (35%) > **14** (21%), in the presence of mismatched DNA than for matched DNA (Figure 4). While it was not possible to directly detect the luminescence of the complexes at room temperature, competition studies provide evidence that the

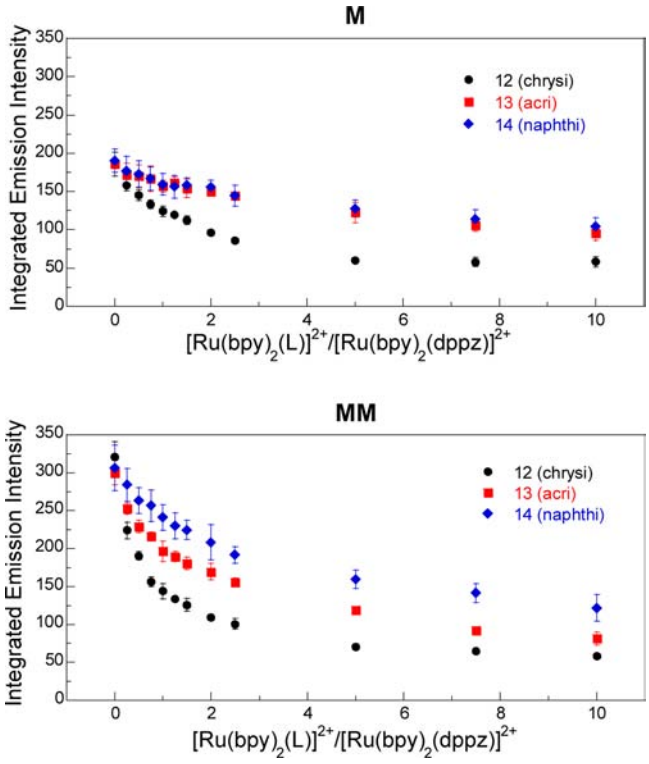

Figure 4. Plots of the integrated emission intensity of 0.1 μM $[Ru(bpy)_2(dppz)]^{2+}$ (**15**) and 0.1 μM matched (M) or mismatched (MM) DNA with up to 10 equiv of $[Ru(bpy)_2(L)]^{2+}$, where L is chrysi (**12**), acri (**13**), or naphthi (**14**) (5 mM Tris, pH 7.5, 50 mM NaCl, λ_{ex} = 440 nm). See Figure 3 for DNA sequences.

dx.doi.org/10.1021/ic3019524 | Inorg. Chem. 2012, 51, 12511–12520

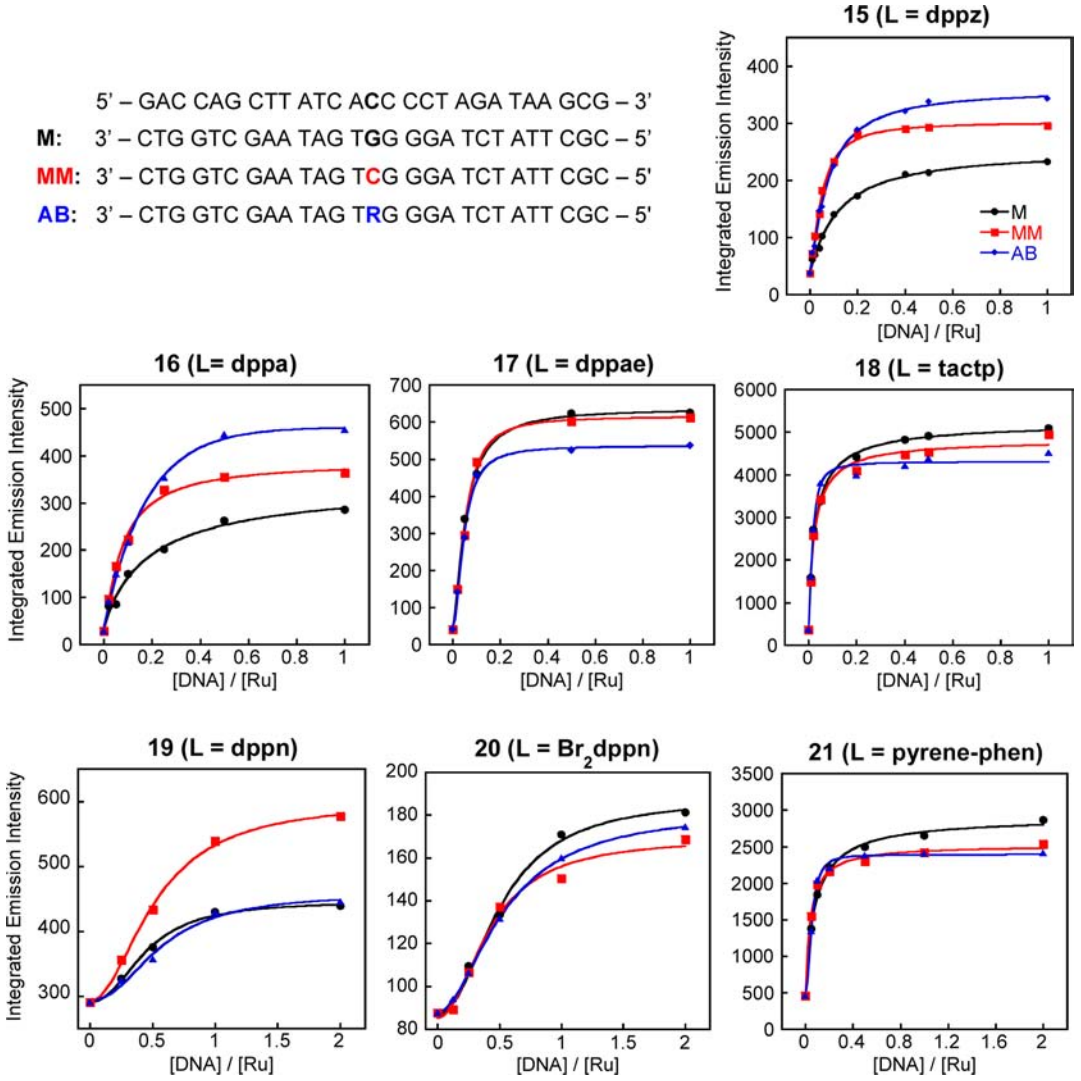

Figure 5. Plots of the integrated emission intensity of **15**–**21** with matched (M), mismatched (MM), and abasic (AB) DNA (5 mM Tris, pH 7.5, 50 mM NaCl, λ_{ex} = 440 nm). [Ru] = 0.1 (for **15**, **18**, and **21**), 1 (for **16** and **17**), 5 (for **19**), and 10 μM (for **20**). DNA sequences are depicted (top, left).

complexes preferentially bind to DNA mismatches through their sterically expansive inserting ligands.

Restoration of luminescence at low temperature for $[Ru(bpy)_2(chrysi)]^{2+}$ (**12**) and $[Ru(bpy)_2(naphthi)]^{2+}$ (**14**) suggests that nonradiative solvent relaxation, most likely through the exchangeable imino protons, is responsible for the loss of luminescence at ambient temperature. Preliminary studies have revealed that methylation of the imino protons of **12** restores luminescence at ambient temperature. However, synthetic difficulties and decomposition of the methylated complex limited further studies.

Unlike complexes **12**–**14**, the $[Ru(bpy)_2(dppz)]^{2+}$ derivatives (**15**–**21**, Figure 2) all show enhanced luminescence with matched (M), mismatched (MM), and abasic (AB) DNA versus in the absence of DNA in aqueous buffer, indicating that the conserved phenazine portion retains some of the photophysical properties of the parent complex **15** (Figure 5). However, complexes having extensively π-conjugated ligands (**18** –**21**) emit luminescence with detectable intensity in the absence of DNA, possibly due to partial shielding of one of the phenazine nitrogens from the solvent by the added steric bulk.

Similar to **15**, the $[Ru(bpy)_2(dppa)]^{2+}$ complex (**16**) exhibits luminescence enhancement in the presence of MM and AB DNA, relative to well-matched DNA, although its binding affinity is lower than that of **15** (Figure 5 and Table S1, Supporting Information). Attachment of a benzo group to the end of the phenazine moiety increases the length of the dppz-type ligand (dppn, Scheme 2). We assume binding to the DNAs resembles that of the dppz complex. Significantly, $[Ru(bpy)_2(dppn)]^{2+}$ (**19**) exhibits an increase in luminescence with MM over M and AB DNA (Figure 5). This may be because the extended dppn ligand of **19**, when bound to well-matched DNA from the major groove, offers less protection to the phenazine nitrogens from solvent water molecules than does dppz. However, for dppn, binding to mismatches likely occurs from the minor groove as it does for dppz. The minor groove is deep and narrow, allowing deeper intercalation of the Ru complex and consequently better protection of the ligand from solvent water.

Introduction of the expansive dppz derivatives dppae and tactp, employing acetylene and chrysene functionalities, respectively, to increase the width of the ligand, eliminates the luminescence differential with DNA defects (Figure 5). In

dx.doi.org/10.1021/ic3019524 | *Inorg. Chem.* 2012, 51, 12511–12520

Table 1. Luminescence Decay Parameters for $Ru(bpy)_2(dppz)^{2+}$ in Competition Experiments with $[Ru(bpy)_2(chrysi)]^{2+}$ (12), $[Ru(bpy)_2(acri)]^{2+}$ (13), and $[Ru(bpy)_2(naphthi)]^{2+}$ (14) in the Presence of Matched (M) and Mismatched (MM) DNA[a]

		M		MM	
complex (ligand)	complex equiv	τ_1, ns (%)[b]	τ_2, ns (%)[b]	τ_1, ns (%)[b]	τ_2, ns (%)[b]
12 (chrysi)	0.0	32 (50)	120 (50)	54 (48)	200 (52)
	0.5	36 (58)	120 (42)	45 (55)	180 (45)
	1.0	36 (64)	120 (36)	36 (54)	140 (46)
	1.5	34 (69)	120 (31)	33 (57)	130 (43)
	2.0	30 (71)	110 (29)	32 (59)	120 (41)
13 (acri)	0.0	37 (40)	120 (60)	48 (46)	190 (54)
	0.5	36 (41)	120 (59)	46 (48)	180 (52)
	1.0	35 (42)	120 (58)	42 (48)	170 (52)
	1.5	36 (45)	120 (55)	41 (50)	170 (50)
	2.0	34 (44)	120 (56)	40 (52)	170 (48)
14 (naphthi)	0.0	37 (40)	120 (60)	46 (43)	180 (57)
	0.5	37 (42)	130 (58)	44 (44)	180 (56)
	1.0	38 (44)	130 (56)	44 (47)	180 (53)
	1.5	36 (44)	120 (56)	45 (50)	180 (50)
	2.0	36 (46)	120 (54)	41 (50)	170 (50)

[a] λ_{ex} = 470 nm, λ_{em} = 610 nm, 5 μM $[Ru(bpy)_2(dppz)]^{2+}$, and 5 μM [DNA] (5 mM Tris, pH 7.5, 50 mM NaCl). Matched (M) and mismatched (MM) oligonucleotides shown in Figure 3 were used. Emission decays were fit to the biexponential function $Y(t) = Y_0 + A_1 \cdot \exp(-t/\tau_1) + A_2 \cdot \exp(-t/\tau_2)$ to give the lifetimes τ_1 and τ_2. Relative contribution of each lifetime to the overall decay is indicated in parentheses. [b] Error is estimated to be ±10%.

the case of $[Ru(bpy)_2(tactp)]^{2+}$ (**18**), a previous study demonstrated that luminescence increases not only through interaction with DNA but also by dimerization or aggregation of the complex itself with or without a DNA template.[8d]

Substituents were also incorporated onto dppn to widen this ligand. These derivatives are Br_2dppn and phen-pyrene (Scheme 2), which are both wider and longer than dppz. Ru complexes (**20** and **21**, Figure 2) bearing Br_2dppn and phen-pyrene do not show any differential luminescence between M, MM, and AB DNA, however (Figure 5). The weak luminescence of **20** may be due to heavy atom quenching by bromine.[29] The increased luminescence of **21** could occur in a manner similar to that of the structural homologue **18**, i.e., through DNA-templated dimerization.[8d]

In summary, the luminescence measurements of **15**–**21** (Figure 2) suggest that structural modification of dppz is not sufficient to improve specific detection of DNA defects through the luminescence response of dppz derivatives. The discrepancy between the high specificity of $[Rh(bpy)_2(chrysi)]^{3+}$ complexes binding to DNA mismatches and the lack of specificity observed for these dppz derivatives might be due to differences in the proximity of the steric bulk to the metal center in the respective complexes. In the $[Ru(bpy)_2(dppz)]^{2+}$ derivatives studied here, the bulky portions of the intercalating ligands are well removed from the metal center, allowing considerable conformational flexibility of binding. In the case of the Rh complex, the chrysi ligand is much closer to the metal center, so its binding geometry is constrained to that imposed by the octahedral center. This notion echoes the conclusions from a previous study comparing the binding of $[Rh(bpy)_2(chrysi)]^{3+}$ to mismatched DNA with that of $[Ru(bpy)_2(eilatin)]^{2+}$.[30] However, unlike the weakly emissive eilatin complex, the dppz derivatives preserve the "light switch" behavior in the presence of DNA.

Excited State Lifetimes. The excited state lifetimes also reveal the binding preferences of the complexes. Given that complexes **12**–**14** (Figure 2) are not luminescent at ambient temperature, their mismatch specificity was investigated through competition experiments with $[Ru(bpy)_2(dppz)]^{2+}$ (**15**) in the presence of matched and mismatched DNA. Luminescence from the dppz complex decays biexponentially, with each lifetime corresponding to one binding geometry: perpendicular (longer lifetime) or side-on (shorter lifetime).[8,16] Greater protection of the phenazine moiety from water via intercalation leads to longer emission lifetimes for the two binding modes (side-on and perpendicular), a higher relative population of the longer-lived species, or both.

The lifetimes do not change within experimental error in the presence of matched DNA upon addition of up to 2 equiv of complexes **12**–**14**, although the relative population of the longer-lived species decreases (Table 1). This is consistent with a change in binding mode from perpendicular to side-on and suggests that the small luminescence decrease observed in the luminescence competition experiments is largely due to a binding mode change rather than displacement of $[Ru(bpy)_2(dppz)]^{2+}$ (**15**) from matched DNA.

In the absence of a competing complex, both lifetimes are greater for a 1:1 mixture of $[Ru(bpy)_2(dppz)]^{2+}$ (**15**) and mismatched DNA compared to well-matched DNA due to greater protection of the phenazine moiety at the mismatch (Table 1). After addition of 2 equiv of complexes **12**–**14**, both excited state lifetimes decrease and approach each of the lifetimes of **15** observed in the presence of matched DNA. The magnitude of the decrease agrees with the steady state luminescence competition experiments where the largest decrease is observed with **12** followed by **13** and **14**. In addition to the lifetime changes, the relative population of the perpendicular state decreases. These results contrast those from analogous experiments with matched DNA, suggesting that the changes are due to displacement of **15** from the mismatch rather than a binding mode change. This is further evidence that the complexes bind preferentially to mismatched DNA over matched DNA.

For the $[Ru(bpy)_2(dppz)]^{2+}$ derivatives (**15**–**21**, Figure 2), the binding preferences of the complexes in 2:1 DNA/Ru mixtures could be probed directly at ambient temperature. As

dx.doi.org/10.1021/ic3019524 | Inorg. Chem. 2012, 51, 12511–12520

shown in Table 2, **15** displays a higher relative abundance bound in the perpendicular mode in the presence of DNA

Table 2. Luminescence Decay Parameters for the $[Ru(bpy)_2(dppz)]^{2+}$ Complexes in the Presence of Matched (M), Mismatched (MM), and Abasic (AB) DNA[a]

	no DNA	in the presence of DNA		
complex (ligand)	τ (ns)[b,c]	DNA	τ_1, ns (%)[c]	τ_2, ns (%)[c]
15 (dppz)	180[d]	M	72 (83)	210 (17)
		MM	74 (77)	210 (23)
		AB	86 (69)	190 (31)
16 (dppa)	190	M	32 (95)	190 (5)
		MM	32 (96)	250 (4)
		AB	26 (93)	540 (7)
17[e] (dppae)	190	M	280 (60)	3900 (40)
		MM	390 (67)	4280 (33)
		AB	500 (62)	4640 (38)
18 (tactp)	210	M	1210 (100)	
		MM	1180 (100)	
		AB	1120 (100)	
19 (dppn)	170	M	62 (51)	840 (49)
		MM	200 (49)	1010 (51)
		AB	35 (58)	710 (42)
20 (Br_2dppn)	200	M	99 (63)	1060 (37)
		MM	130 (66)	880 (34)
		AB	82 (54)	800 (46)
21 (pyrene-phen)	190	M	930 (100)	
		MM	880 (100)	
		AB	810 (100)	

[a] λ_{ex} = 470 nm, λ_{em} = 610 nm, 10 μM [Ru], and 20 μM [DNA] (5 mM Tris, pH 7.5, 50 mM NaCl). Matched (M), mismatched (MM), and abasic (AB) oligonucleotides in Figure 5 were used. Emission decays were fit to the monoexponential function $Y(t) = Y_0 + A_1 \cdot \exp(-t/\tau_1)$ or biexponential function $Y(t) = Y_0 + A_1 \cdot \exp(-t/\tau_1) + A_2 \cdot \exp(-t/\tau_2)$ to give the lifetimes τ_1 and τ_2. Relative contribution of each lifetime to the overall decay is indicated in parentheses. [b] [Ru] = 10 μM, CH_3CN. [c] Error is estimated to be ±10%. [d] Reference 8. [e] 20 μM [Ru] and 40 μM [DNA].

following the order AB > MM > M. This supports the observation from steady state measurements that the luminescence intensity of **15** is present in the following order: AB > MM > M (Figure 5).[16] Likewise, in the case of $[Ru(bpy)_2(dppa)]^{2+}$ (**16**), longer lifetimes corresponding to the perpendicular mode (AB > MM > M) are observed, which can explain the trend in the steady state luminescence measurements of **16**, as shown in Figure 5. Furthermore, $[Ru(bpy)_2(dppn)]^{2+}$ (**19**), which shows differential luminescence turn-on with MM over M and AB, indicates longer lifetimes in both binding modes only with MM. Overall, excited state lifetime measurements indicate that **15**, **16**, and **19** display longer lifetimes or a higher population in the perpendicular mode in the presence of DNA containing a lesion, suggesting greater protection of the phenazine nitrogen atoms upon binding to DNA defects.

Ru complexes **18** and **21**, which can aggregate in the presence of a DNA template, exhibit single-exponential luminescent decays with DNA (Table 2), suggesting that their luminescence enhancement originates mainly from nonspecific binding to DNA. Ru complexes **17** and **20**, which have increased steric bulk on the phenazine fragment but utilize different substituents than **18** and **21**, present biexponential decays in emission. Lifetime measurements show a lower relative yield of long-lived species for **17** and shorter lifetimes for **20** in the presence of DNA-containing defects. These results are consistent with the slight decrease in steady state luminescence observed for **17** and **20** when combined with DNA-containing defects (Figure 5).

SUMMARY AND IMPLICATIONS

Taking inspiration from the mismatch specificity of the sterically expansive chrysi ligand and light switch behavior of $[Ru(bpy)_2(dppz)]^{2+}$, a family of Ru(II) complexes was prepared in an attempt to specifically target DNA defects and indicate their presence by the appearance of luminescence. In one design strategy, complexes containing sterically expansive ligands, such as chrysi and analogues with hydrogen-bonding functionality similar to dppz, were synthesized. Incorporation of the sterically expansive ligand appears to improve the mismatch specificity; however, the complexes are nonluminescent at room temperature. The exchangeable imino protons most likely quench luminescence at room temperature through solvent relaxation as luminescence is restored at 77 K for $[Ru(bpy)_2(chrysi)]^{2+}$ (**12**) and $[Ru(bpy)_2(naphthi)]^{2+}$ (**14**). Despite their mismatch specificity, the lack of luminescence signals at room temperature limits the use of these complexes as probes. Light switch behavior cannot be exploited at low temperature to improve mismatch discrimination, as the known "light switch" complex $[Ru(bpy)_2(dppz)]^{2+}$ (**15**) shows luminescence at 77 K even in the absence of DNA.

Ru complexes containing dppz derivatives (**15**–**21**) were also synthesized with the goal of increasing their steric bulk through incorporation of various functionalities on the ligand framework. Their luminescence responses, however, were not substantially enhanced compared with the parent complex **15** in the presence of DNA with a mismatched or abasic site. Nevertheless, the narrow ligands (dppa and dppn) show differential luminescence behavior in the presence of a DNA defect. Widening the dppz ligand using a simple group such as acetylene or Br does not enhance targeting to destabilized regions of DNA. Furthermore, Ru complexes with the extensively π-conjugated ligands (tactp and pyrene-phen) are likely to aggregate and are therefore unable to report mismatches via luminescence output.

These observations are consistent with a recent crystal structure in which the dppz ligand of Δ-$[Ru(bpy)_2(dppz)]^{2+}$ inserts deeply from the minor groove at mismatched sites.[14] In the crystal structure, the central ring of the phenazine portion of dppz stacks with the DNA bases, affording the nitrogen atoms of the phenazine moiety maximum protection from solvent water. Considering the structural resemblance between dppa and dppz, complexes of the two ligands are likely to bind DNA in the same manner. The similarity in mismatch discrimination between $[Ru(bpy)_2(dppa)]^{2+}$ (**16**) and $[Ru(bpy)_2(dppz)]^{2+}$ (**15**) is therefore not surprising. Extension of dppz to form dppn alters the equilibrium binding geometry of the complex. The relatively high mismatch discrimination of the dppn complex may therefore indicate stronger binding and more effective protection from solvent at mismatched sites. Similarly, widening the terminal phenazine ring of dppz to form tactp or pyrene-phen may result in stacking between the DNA bases and these wider, extended structures, decreasing the degree of protection experienced by the nitrogen atoms of the phenazine ring. Presumably, these modifications are also responsible for aggregation of the complexes. Consequently,

dx.doi.org/10.1021/ic3019524 | Inorg. Chem. 2012, 51, 12511–12520

the phenazine nitrogens in tactp and pyrene-phen may be similarly accessible to solvent whether the complex is dimerized, intercalated, or inserted; hence, the tactp and pyrene-phen complexes exhibit similar luminescence profiles with all three types of DNA.

Of the two approaches investigated here, increasing the steric bulk of the dppz framework appeared to be more successful, as all of the derivative complexes retained "light switch" behavior. Although the structural modifications investigated here are not sufficient by themselves to enhance the luminescence differential between matched and defective DNA, future efforts to improve the mismatch specificity of $[Ru(bpy)_2(dppz)]^{2+}$ should perhaps shift away from appending steric bulk to the distal portion of the dppz ligand. The $[Ru(bpy)_2(dppz)]^{2+}$ scaffold, thus, may be able to withstand the even bolder modifications necessary to achieve mismatch-specific luminescence.

■ ASSOCIATED CONTENT

Ⓢ Supporting Information

Chemical structure and characterization information of $[Ru(bpy)_2(iqi)]^{2+}$ (**22**), Tables S1 and S2, and Figures S1−S3. This material is available free of charge via the Internet at http://pubs.acs.org.

■ AUTHOR INFORMATION

Corresponding Author

*E-mail: jkbarton@caltech.edu.

Present Address

[†]Life Sciences Institute and Department of Chemistry, University of Michigan, Ann Arbor, MI 48109, United States.

Notes

The authors declare no competing financial interest.

■ ACKNOWLEDGMENTS

We thank the NIH (GM33309 to J.K.B.) for their financial support, the Lindemann Trust for a postdoctoral fellowship to A.J.M., the Tobacco-Related Disease Research Program (TRDRP) for a postdoctoral fellowship to M.H.L., and a Dissertation Research Award to H.S. We also thank Dr. Eva Rüba for developing the synthesis of $[Ru(bpy)_2(chrysi)]^{2+}$ and Jessica Yeung for carrying out preliminary studies. We are grateful to the Beckman Institute Laser Resource Center (BILRC) at Caltech for facilities.

■ REFERENCES

(1) Hoeijmakers, J. H. *Nature* **2001**, *411*, 366−374.
(2) Jiricny, J. *Nat. Rev. Mol. Cell Biol.* **2006**, *7*, 335−346.
(3) Lovett, S. T. *Mol. Microbiol.* **2004**, *52*, 1243−1253.
(4) Zeglis, B. M.; Pierre, V. C.; Barton, J. K. *Chem. Commun.* **2007**, *44*, 4565−4579.
(5) (a) Jackson, B. A.; Barton, J. K. *J. Am. Chem. Soc.* **1997**, *119*, 12986−12987. (b) Jackson, B. A.; Alekseyev, V. Y.; Barton, J. K. *Biochemistry* **1999**, *38*, 4655−4662. (c) Jackson, B. A.; Barton, J. K. *Biochemistry* **2000**, *39*, 6176−6182.
(6) Hart, J. R.; Glebov, O.; Ernst, R. J.; Kirsch, I. R.; Barton, J. K. *Proc. Natl. Acad. Sci. U.S.A.* **2006**, *103*, 15359−15363.
(7) Zeglis, B. M.; Barton, J. K. *J. Am. Chem. Soc.* **2006**, *128*, 5654−5655.
(8) (a) Friedman, A. E.; Chambron, J. C.; Sauvage, J. P.; Turro, N. J.; Barton, J. K. *J. Am. Chem. Soc.* **1990**, *112*, 4960−4962. (b) Jenkins, Y.; Friedman, A. E.; Turro, N. J.; Barton, J. K. *Biochemistry* **1992**, *31*, 10809−10816. (c) Hartshorn, R. M.; Barton, J. K. *J. Am. Chem. Soc.* **1992**, *114*, 5919−5925. (d) Rüba, E.; Hart, J. R.; Barton, J. K. *Inorg. Chem.* **2004**, *43*, 4570−4578.
(9) (a) Pierre, V. C.; Kaiser, J. T.; Barton, J. K. *Proc. Natl. Acad. Sci. U.S.A.* **2007**, *104*, 429−434. (b) Cordier, C.; Pierre, V. C.; Barton, J. K. *J. Am. Chem. Soc.* **2007**, *129*, 12287−12295. (c) Zeglis, B. M.; Pierre, V. C.; Kaiser, J. T.; Barton, J. K. *Biochemistry* **2009**, *48*, 4247−4253.
(10) Zeglis, B. M.; Boland, J. A.; Barton, J. K. *J. Am. Chem. Soc.* **2008**, *130*, 7530−7531.
(11) Hiort, C.; Lincoln, P.; Nordén, B. *J. Am. Chem. Soc.* **1993**, *115*, 3448−3454.
(12) Brennaman, M. K.; Meyer, T. J.; Papanikolas, J. M. *J. Phys. Chem. A* **2004**, *108*, 9938−9944.
(13) (a) Dupureur, C. M.; Barton, J. K. *J. Am. Chem. Soc.* **1994**, *116*, 10286−10287. (b) Dupureur, C. M.; Barton, J. K. *Inorg. Chem.* **1997**, *36*, 33−43.
(14) Song, H.; Kaiser, J. T.; Barton, J. K. *Nat. Chem.* **2012**, *4*, 615−620.
(15) Niyazi, H.; Hall, J. P.; O'Sullivan, K.; Winter, G.; Sorensen, T.; Kelly, J. M.; Cardin, C. J. *Nat. Chem.* **2012**, *4*, 621−628.
(16) Lim, M. H.; Song, H.; Olmon, E. D.; Dervan, E. E.; Barton, J. K. *Inorg. Chem.* **2009**, *48*, 5392−5397.
(17) Zeglis, B. M.; Barton, J. K. *Nat. Protoc.* **2007**, *2*, 357−371.
(18) Sullivan, B. P.; Salmon, D. J.; Meyer, T. J. *Inorg. Chem.* **1978**, *17*, 3334−3341.
(19) Dickeson, J. E.; Summers, L. A. *Aust. J. Chem.* **1970**, *23*, 1023−1027.
(20) Brunner, J.; Barton, J. K. *Biochemistry* **2006**, *45*, 12295−12302.
(21) Martinez, R.; Ramon, D. J.; Yus, M. *J. Org. Chem.* **2008**, *73*, 9778−9780.
(22) Thomas, A. A.; Le Huerou, Y.; De Meese, J.; Gunawardana, I.; Kaplan, T.; Romoff, T. T.; Gonzales, S. S.; Condroski, K.; Boyd, S. A.; Ballard, J.; Bernat, B.; DeWolf, W.; Han, M.; Lee, P.; Lemieux, C.; Pedersen, R.; Pheneger, J.; Poch, G.; Smith, D.; Sullivan, F.; Weiler, S.; Wright, S. K.; Lin, J.; Brandhuber, B.; Vigers, G. *Bioorg. Med. Chem. Lett.* **2008**, *18*, 2206−2210.
(23) Avnir, D.; Blum, J. *J. Heterocycl. Chem.* **1976**, *13*, 619−621.
(24) DaSilveira Neto, B. A.; Sant'Ana Lopes, A.; Ebeling, G.; Gonçalves, R. S.; Costa, V. E. U.; Quina, F. H.; Dupont, J. *Tetrahedron* **2005**, *61*, 10975−10982.
(25) Yang, J.; Jiang, C.; Zhang, Y.; Yang, R.; Yang, W.; Hou, Q.; Cao, Y. *Macromolecules* **2004**, *37*, 1211−1218.
(26) Bodige, S.; MacDonnell, F. M. *Tetrahedron Lett.* **1997**, *38*, 8159−8160.
(27) Inglett, G. E.; Smith, G. F. *J. Am. Chem. Soc.* **1950**, *72*, 842−844.
(28) Sodium hydride is necessary for the condensation reaction to proceed; however, similar yields were obtained, reducing the number of equivalents of sodium hydride.
(29) Dreeskamp, H.; Koch, E.; Zander, M. *Chem. Phys. Lett.* **1975**, *31*, 251−253.
(30) Zeglis, B. M.; Barton, J. K. *Inorg. Chem.* **2008**, *47*, 6452−6457.